JURNAL ILMU LINGKUNGAN
Volume 23 Issue 2 (2025) : 452-462 *ISSN 1829-8907*

The Study of Coastal Vulnerability in North Insana District, North Central Timor Regency, East Nusa Tenggara Province (Indonesia)

Ludgardis Ledheng[1*], Blasius Atini[1], and Emanuel Maria Yosef Hano'e[1]

[1]Biology Education Study Program, Faculty of Teacher Training and Educational Sciences Timor University, Kefamenanu, Indonesia; e-mail: ludgardisledheng12@gmail.com

ABSTRAK

Berkurangnya kawasan mangrove yang menyebabkan erosi signifikan di sepanjang pantai utara Kabupaten Timor Tengah Utara, menyiratkan perlunya kajian mendalam. Penelitian ini bertujuan untuk mengetahui sebaran spasial kerentanan pesisir dan faktor-faktor yang mempengaruhinya dengan menggunakan Coastal Vulnerability Index (CVI). Hasil penelitian menunjukkan bahwa sepanjang 7,07 km (48,71%) garis pantai tergolong kerentanan rendah, sedangkan 6,66 km (51,28%) tergolong sedang. Faktor-faktor kunci yang mempengaruhi kerentanan pesisir meliputi geomorfologi (87,18%), perubahan garis pantai (7,6%), kemiringan pantai (66,6%), dan ketinggian pantai (66,7%), berdasarkan pengamatan di 39 sel. Sementara itu, variabel pasang surut, tinggi gelombang, dan kenaikan permukaan air laut mempunyai dampak yang minimal, dan tingkat kerentanan yang terkait termasuk dalam kategori rendah. Penelitian di masa depan harus memasukkan variabel tambahan, seperti aspek sosio-ekonomi dan aktivitas manusia untuk memberikan penilaian yang lebih komprehensif mengenai kerentanan pesisir. Hal ini akan menghasilkan penilaian yang lebih holistik dalam pengambilan keputusan perencanaan mitigasi wilayah pesisir.

Kata kunci: Kerentanan, Pesisir**,** Geologi, Variabel proses fisik, Insana Utara

ABSTRACT

The reduction in mangrove areas, which has caused significant erosion along the north coast of North Central Timor Regency, has implied the need for in-depth studies. This research, aimed to determine the spatial distribution of coastal vulnerability and its influencing factors using the Coastal Vulnerability Index (CVI). The research found that 7.07 km (48.71%) of the coastline was classified as low vulnerability, while 6.66 km (51.28%) was categorized as moderate. Key factors influencing coastal vulnerability include geomorphology (87.18%), coastline changes (7.6%), beach slope (66.6%), and beach elevation (66.7%), based on observations across 39 cells. Meanwhile, tidal variables, wave height, and sea-level rise had minimal impact, with their associated vulnerability levels categorized as low. Future research should incorporate additional variables, such as socio-economic aspects and human activities to provide a more comprehensive assessment of coastal vulnerability. This would result in a more holistic assessment for decision-making for coastal area mitigation planning.

***Keywords*:** Coastal, Vulnerability, Geology, Physical process variables, North Insana

Citation: Ledheng, L., Atini, B., dan Hano'e, E. M. Y. (2025). The Study of Coastal Vulnerability in North Insana District, North Central Timor Regency, East Nusa Tenggara Province (Indonesia). Jurnal Ilmu Lingkungan, 23(2), 452-462, doi:10.14710/jil.23.2.452-462

1. INTRODUCTION

Coastal areas are rich in biological and non-biological resources, which support high economic activity and place significant pressure on coastal spaces (Febriansyah, Agus & Helmi, 2012). In Indonesia, efforts to protect, preserve, and utilize coastal areas are regulated in the Regulation of the Minister of Maritime Affairs and Fisheries of the Republic of Indonesia number 23, 2016. One of the first steps in a coastal management plan is identifying the physical problems occurring in coastal areas, as coastal areas are highly sensitive and vulnerable to natural phenomena. According to Suhana *et al*. (2020), coastal areas are vulnerable to environmental factors such as climate change and sea-level rise. The impacts of these phenomena on coastal areas need to be studied, especially through identifying the spatial distribution of coastal vulnerability. Factors that influence coastal vulnerability assessment include geomorphology, rate of change of shoreline, beach slope, elevation, sea-level rise, tides, and wave height (Rumahorbo, Warpur, Tanjung, & Hamuna, 2023).

Several studies have examined the degree of vulnerability in coastal areas in Indonesia. Sakka,

Paharuddin & Rupang, (2014), for instance, assessed coastal susceptibility in Makassar City and found that base slope and shoreline changes were the key parameters that greatly influenced coastal vulnerability. A study conducted in Papua Province by Hamuna, Sari & Alianto, (2018) identified geomorphology and elevation as the primary factors affecting coastal vulnerability in Jayapura City. Meanwhile, a study in Semarang City by Karondia, Handoko, and Handayani (2022) confirmed that sea-level rise was a significant contributor to coastal vulnerability. These studies provided insights into the vulnerability of coastal areas in Indonesia.

Most coastal areas, including those in East Nusa Tenggara Province, particularly the coast of North Central Timor (NCT) Regency, face significant pressures and changes. The North Insana District coastline, as a key area for coastal development in NCT Regency, has been heavily impacted by human activities. Ledheng, Ardhana, & Sundra (2012) found that human activities along the North Insana District coast have caused a significant decline in mangrove populations. This reduction in mangrove area is partly attributed to the utilization of coastal space for various purposes, including road infrastructure, housing, and aquaculture (Ledheng *et al*., 2012). The decrease in mangrove vegetation has also led to a decrease in species composition. In 2009, 29 mangrove species were recorded along the north coast of NCT Regency (Ledheng *et al*., 2012). This number had decreased to just four species by 2020 (Ledheng, Naisumu, & Binsasi, 2020). Damage and disturbance to mangrove growth strata has hindered the regeneration process of mangrove trees. The results of a recent study conducted by Ledheng & Hano'e (2023) showed that most of the north coast of NCT Regency experienced shoreline abrasion, with the most significant change of shoreline 549 meters happening in North Insana District. This condition has become a threat, especially to the coast of North Insana District, underscoring the need for a study to map and examine coastal vulnerability using the Coastal Vulnerability Index (CVI). Such research aims to provide an initial overview of the coastal threats in the North Insana District, especially those arising from sea-level rise driven by climate change.

2. METHODS

2.1. Time and Location

This research was conducted from March to August 2023 along the north coast of North Central Timor Regency, East Nusa Tenggara Province. The research area covered 13.71 km of coastline, with a total number of 39 cells, each measuring 400 m x 400 m (Figure 1). The research took place in Wini Village and Oesoko Village, North Insana District. These locations were selected based on several factors, including high levels of coastal tourism activity, the development of highways infrastructure, and the expansion of aquaculture, all of which have contributed to increased space utilization. A map of the research locations is presented in Figure 1.

2.2. Data Collection

This study utilized seven variables to examine the level of coastal vulnerability: beach elevation, beach slope, geomorphology, shoreline changes, tidal range, wave height, and sea level height. Most of these variables were based on secondary data, with field observation beforehand as a validation process, especially for geomorphology, beach slope, elevation, and shoreline changes. This study gathered the data of elevation and slope from the Digital Elevation Model Nasional (DEMNAS) produced by the Indonesian Geospatial Information Agency, as accessible at https://tanahair.indonesia.go.id/demnas. The DEMNAS data was obtained from various data sources, including IFSAR and TERRASAR-X data with 5 m resolution, as well as ALOS PAL-SAR with an 11.25 m resolution. Additionally, mass-point data were incorporated from stereo-plotting.

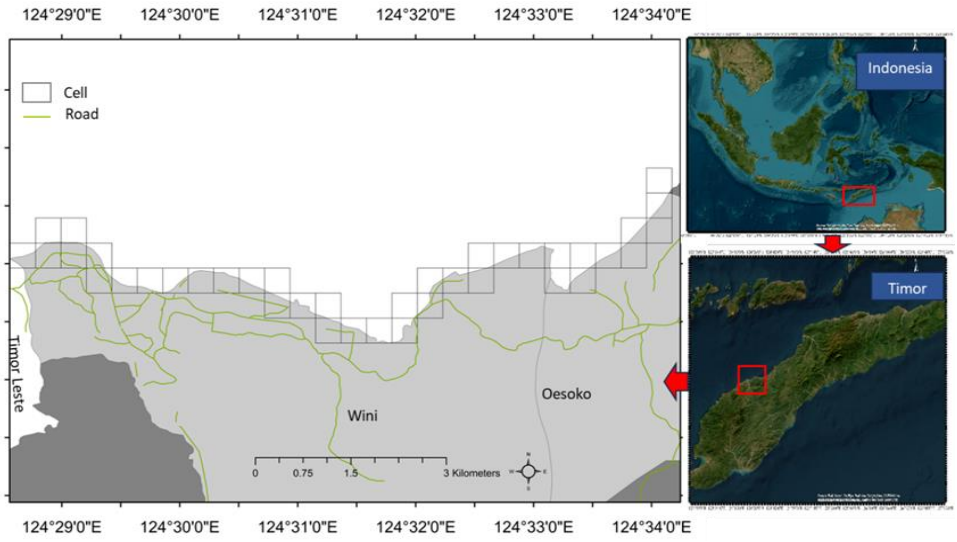

Figure 1. Research Location

Table 1. Types of Tides Based on the Value of Formzahl Number (F)

The Criteria of Formzahl Number	Type of Tides
F ≤ 0.25	Semidiurnal
0.25 ≤ F ≤1.5	Mixed Semidiurnal
1.5 ≤ F ≤ 3.0	Mixed Diurnal
F > 3.0	Diurnal

To process the data, six DEM data files were combined into a single file through an image mosaic operation, ensuring integration. The final file was saved using the Universal Transverse Mercator projection system (UTM 51S) and the World Geodetic System (WGS84) datum. The DEM data was then clipped to match the study area boundaries of the North Insana District, using shapefile (SHP) format to create polygon features, to generate elevation and slope data. Finally, the whole DEM data were analyzed spatially using ArcGis 10.8.1 software that produce maps of elevation vulnerability and coastal slope.

The geomorphological data were gathered from land cover maps processed using Indonesian-based datasets (Hamuna *et al*., 2018). Shoreline change data were obtained from an analysis of Landsat 8 imagery recorded on 2014-09-09 and 2023-05-13. The analysis utilized ENVI software for shoreline extraction and the Digital Shoreline Analysis System (DSAS), integrated with ArcGis 10.8.1. The shoreline change was calculated using the DSAS output, especially the End Point Rate (EPR) method.

Tidal data were obtained from the results of the MIKE 21 software forecasting for the periods 2014, 2017, 2020, 2021, and 2023. Tidal types and characteristics were calculated using the Formzahl equation:

$$F = \frac{K1+O1}{M2+S2} \quad (1)$$

where:

F : Formzahl
O1 : The principal diurnal tidal constituent caused by the Moon's gravity
K1 : The principal diurnal tidal constituent influenced by the Sun's gravity
M2 : The principal semidiurnal tidal constituent caused by the Moon's gravity
S2 : The principal semidiurnal tidal constituent influenced by the Sun's gravity

The calculation of Tidal Range (TR) follows the method proposed by Suhana *et al*. (2016), assuming a Mean Sea Level (MSL) value of 0. The equations used are as follows:

$$MHWS = MSL+((M2+Ki+O1)/2) \quad (2)$$
$$MHWN = MSL+((Ki+O1-m2)/2) \quad (3)$$
$$MLWN = MSL-((Ki+O1-m2)/2) \quad (4)$$
$$MLWN = MSL-((Ki+O1+m2)/2) \quad (5)$$
$$TRS = MHWS-MLWS \quad (6)$$
$$TRN = MHWN-MLWN \quad (7)$$
$$TR = TRS-TRN \quad (8)$$

where:

MHWS : Mean High Water Springs.
MHWN : Mean High Water Neaps.
MHWN : Mean High Water Neaps.
MLWS : Mean Low Water Springs.
TRS : Tidal Range Springs.
TRN : Tidal Range Neaps.
TR : Tidal Range.

The Copernicus Program was used to obtain wave height and sea level data, accessible at https://cds.climate.copernicus.eu/about-3s. Wave height data from the site included wind direction and wind speed, which were then converted into wave height values. Meanwhile, sea-level rise data were extracted from https://cds.climate.copernicus.eu/about-3s in NetCDF (.nc) format and processed using Ocean Data View (ODV) software to convert them into text (.txt) format. The *.txt data were then interpolated using Surfer 9 software. Next, the interpolation results were cropped to match the study area and exported as *.xyz format data using Global Mapper 9. The final process was assigning the closest value to the coast line cells. An overlay was then conducted with the shoreline cells, and the data were digitized using Surfer 9.

2.3. Data Analysis

To obtain the vulnerability indicators, the CVI values for the coastal area in North Insana District were calculated by incoporating the values of the seven variables used in this study. The determination of vulnerability for elevation followed the methodology of Pendleton *et al*. (2010), while that for wave height referred to Jadidi *et al*. (2013). Furthermore, the other variables, namely coastal slope, geomorphology, shoreline changes, tidal range, and sea level, were assessed based on the framework suggested by Pendleton *et al*. (2010). This reference was deemed ideal for the study location due to its applicability to archipelagic regions. The CVI values for the seven variables were categorized into five groups: very low, low, moderate, high, and very high (Table 3). The CVI calculation referred to the formula proposed by Pendleton *et al*. (2010):

$$CVI = \frac{\sqrt{a*b*c*d*e*f*g}}{n} \quad (9)$$

where:

a = coastal geomorphology
b = beach slope
c = abrasion/accretion
d = tidal range
e = elevation
f = sea surface height
g = wave height
n = total number of variables
CVI = Coastal Vulnerability Index

The CVI value of coastal vulnerability was grouped into four categories according to Pendleton *et al*. (2010), as presented in Table 3.

Table 2. Categories and Weighting of CVI Variable Scores

Variable	Very Low	Low	Moderate	High	Very High
	1	2	3	4	5
Geomorphology	High cliffs, vegetation	Moderate cliffs, vegetation	Low cliffs, alluvial plains, vegetation	Cobble beaches, estuary, lagoon, vegetation	Barrier beaches, sand beaches, salt marshes, mud flats, deltas, vegetation, coral reefs
Shoreline change (m/year)	> 2.0	1.0–2.0	-1.0–1.0	-2.0–-1.0	<-2.0
Mean tidal range (m)	< 1.0 microtidal	1.0–1.9 microtidal	2.0–4.0 mesotidal	4.1-6.0 macrotidal	> 6.0 macrotidal
Coastal slope (%)	> 14.7	10.9–14.69	7.75–10.89	4.6–7.74	<4.59
Elevation (m)	> 30	20.1–30	10.1–20	5.1–10	<5
Relative sea-level rise (mm/year)	1.8	1.81–2.5	2.51–3.0	3.01–3.4	>3.4
Mean wave height (m)	<0.5	0.5–1.0	1.0–1.5	1,5–2.0	>2.0

Table 3. Groups of CVI

Score	Category
<4.75	Low
4.75-10.64	Medium
10.64-19.66	High
>19.66	Very High

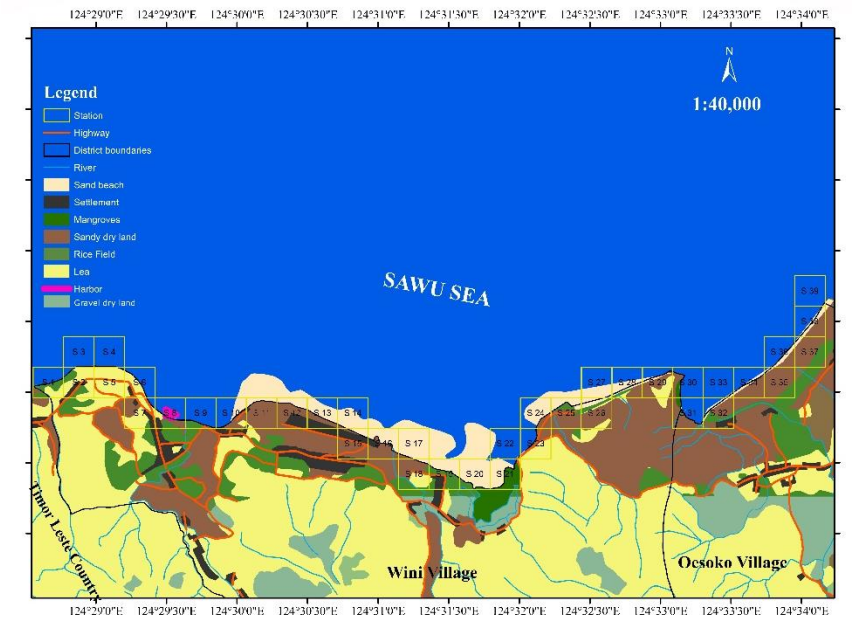

Figure 2. Geomorphological Appearance

3. RESULTS AND DISCUSSION

3.1. Geomorphology

The coastal land in North Insana District consists of sandy dry land, meadow, gravel dry land, rice fields, sand beaches, mangrove vegetation on rocky land, and settlements (Figure 2). In general, the coastal landscape appearance of North Insana District is predominantly composed of sandy dry land. Salt production activities take place on the sandy dry land, where the sand is used as raw material for salt production, as observed in cell 32 in Oesoko Village. Coastal development in North Insana District is more prominent in Wini Village, which includes the construction of highway infrastructure (cells 15, 21, 22, and 23) (Figure 2), beach tourism areas (cell 6), and a horserace track (cell 24). This development has negatively impacted mangrove vegetation, leading to extinction. Laming and Rahim (2020) also stated that coastal development often has a negative impact on the environment, requiring serious attention from policymakers. The condition of the mangrove vegetation was monitored at cells 20 and 21. However, the vegetation in cell 21, adjacent to the road, has been damaged. This was confirmed, as confirmed by shoreline changes indicating road encroachment and vegetation damage (Figure 5). The morphology of cell 21 was categorized as low vulnerability due to its rocky beach, while cells 22, 23, 29, and 30 were classified having very low vulnerability because the coastal slopes were hilly and contained numerous rocks that could block sea waves.

According to Ledheng & Hano'e (2023), the northern coastal area of North Central Timor Regency features two adjacent accumulations of sand deposits: sand transported by tidal movements and sand carried by river flows. This causes sandy dry land dominating the coastline. Yuliastini, Zainuri, and Widiaratih (2023) classified sandy dry land as the alluvial plains category, which is prone to coastal abrasion. The vulnerability index of geomorphological parameters along the coast of North Insana District is presented in Figure 3.

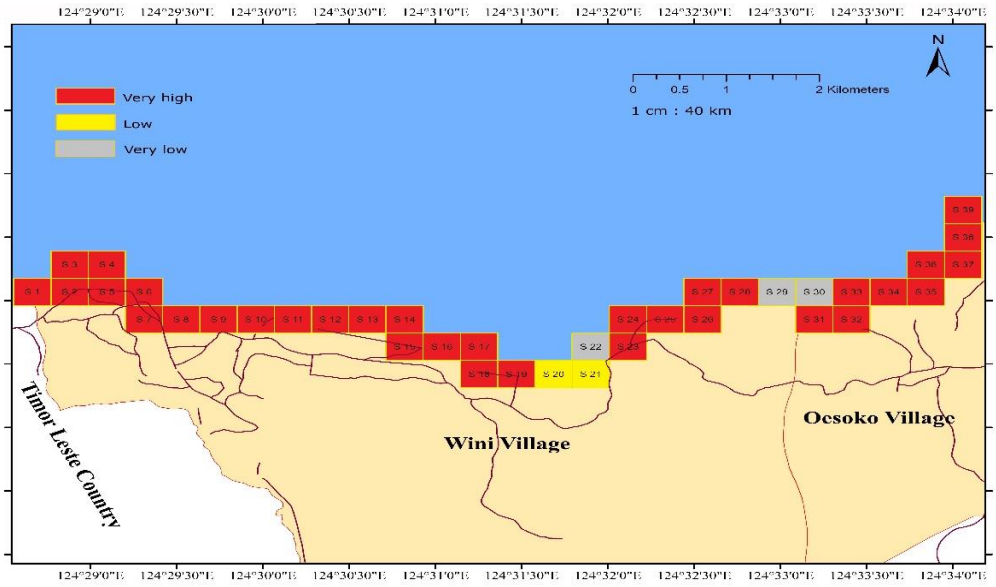

Figure 3. Vulnerability Categories based on Geomorphology

Based on Figure 3, among the 39 cells observed, areas classified as having very high vulnerability accounted for 87.18%, while those with low and very low vulnerability represented 5.13% and 7.69%, respectively. The dry sandy land in North Insana District is predominantly composed of tidal flats. Geomorphological characteristics in areas with average tidal activity increase the potential for vulnerability; however, areas covered by mangroves are relatively safe from coastal abrasion threats. The ability of forests to maintain the balance of sediment transport helps mitigate the risk of coastal erosion (Siregar *et al*., 2016).

3.2. Shoreline Change

The results of the DSAS analysis showed that the rate of abrasion between 2014 and 2023 along the coast of North Insana District was 1.2 m/year, while the accretion rate was 2.1 m/year. In general, shoreline changes were primarily observed in residential areas, locations near highways, horseracing tracks, and aquaculture ponds. The vulnerability indexes ranged from very low to very high category. Areas experiencing sedimentation were found to have very low vulnerability. Cells categorized as having high vulnerability on Wini Beach were areas near settlements (cells 3–8, 16), mangrove areas adjacent to highways (cell 21), and near the horseracing track (cells 24, 26–28). On Oesoko Beach, high vulnerability was observed in the conservation area (cell 31) and near the ponds (cell 33). The highest vulnerability was found in the Oesoko coast, namely in cells 32 and 35–36 (Figures 7). The impact of the Seroja storm in 2021 caused the coast of Oesoko (cells 31 and 32) to experience a shoreline shift of 567 m (Ledheng & Hano'e, 2023). This prompted village and district governments to initiate a mangrove seedling planting program and designate the area as a conservation zone. The Oesoko coast as an area with a flat slope and small daily waves requires protection as a conservation area, as, according to Nurrohmah *et al*. (2016), areas with high waves are unsuitable for conservation purposes. Despite the designation of cell 31 as a conservation area, it remains classified as having high vulnerability (Figure 4). Cells 35–36 on the Oesoko coast, moreover, showed high vulnerability due to the dominance of sandy terrain without vegetation and the flat beach slope (Figure 4).

The shoreline with stable changes was found near the border post of Timor Leste State and Indonesia (cells 1–2) and in residential areas (cells 9–15, 17, and 19). The most stable shorelines were observed in the mangrove area (cell 20), areas experiencing high sedimentation (cells 29-30), and in cells 37-39 along the Oesoko coast (Figure 4). Based on Figure 4, among the 39 cells observed, the vulnerability criteria were classified as moderate, high, and very high, at 38.46%, 25.64%, and 7.69, respectively.

3.3. Sea Tides

The maximum sea surface height at the highest tide, based on field measurements in July 2022, was 151 cm, while the minimum height at the lowest tide was 26 cm, with an average sea level surface (MSL) of 125 cm (Ledheng & Hano'e, 2023). Validation of these field measurements showed a consistent sea level elevation pattern, despite differing elevation values. The validation using the MIKE 21 prediction in July 2023 showed that the sea surface height at the highest tide was 149 cm, and the minimum height at the lowest tide was 24 cm (Figure 5).

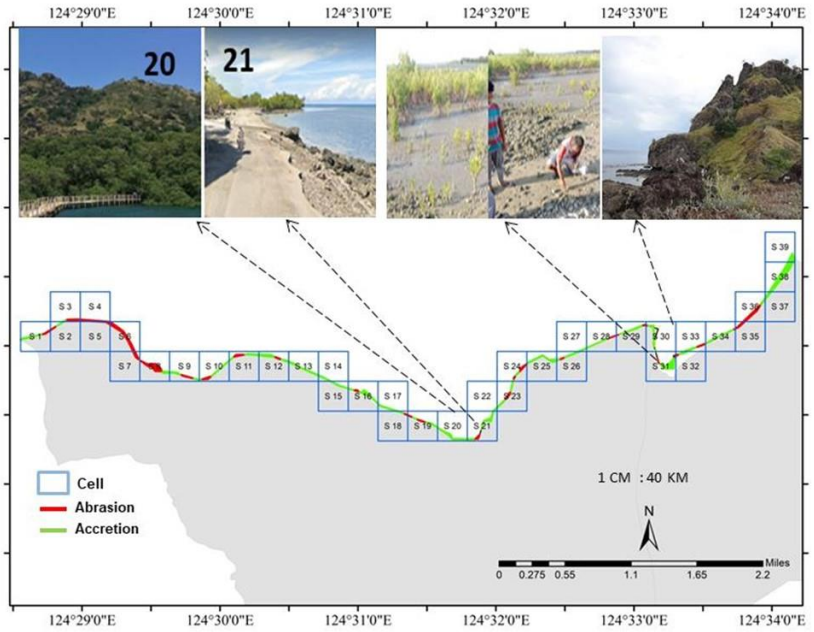

Figure 4. Map of Abrasion and Accretion of North Insana District in 2014 - 2023

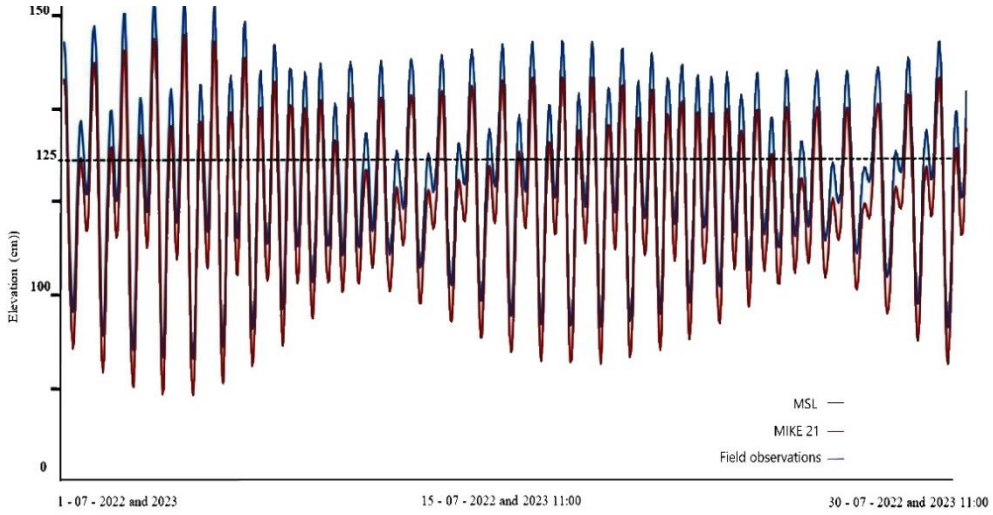

Figure 5. The Tidal Pattern Observed from Field Measurements in July 2022 and the MIKE Predictions on July 21, 2023

Table 4. The Results of the 2023 Tidal Analysis on Coastal Vulnerability

MHHWS	MHHWN	TR	Scor CVI	Vulnerability Category
53.82	8.52	125	2	Low Vulnerability

Notes: MHHWS = mean highest of high-water spring; MHHWN = mean highest of high-water neap; TR = tidal range

The tidal analysis performed in North Insana beach in July 2023 suggested that the maximum sea surface height during spring tide reached 53.82 cm, while during neap tide, it was 8.52 cm, with a tidal range of 125 cm classifying this area as microtidal based on Dipper's category (2022). The mean tide height depicts the difference between the average heights of the highest and the lowest tides. According to Pendleton *et al*. (2010), the average slope value plays an important role in coastal vulnerability, as tidal range contributes to the periodic inundation of coastal areas. The vulnerability index value based on tidal range in the coast of North Insana over the past decade indicates that all 39 cells (100%) observed were categorized vulnerable. Based on analysis using MIKE 21, the tidal type in North Insana waters is a mixed diurnal-inclined pattern, with a Formzhal number of 0.48, falling within the range of 0.25 to 1.50. this tidal type is characterized by two high and two low tides each day, with one being more dominant. These findings highlight the dynamic tidal influences affecting coastal vulnerability in the region.

3.4. Slope and Elevation

The slope class of North Insana beach consists of flat slopes, gentle slopes and very steep slopes. Flat slopes on the Wini coast ranged from 0.05% to 1.58% and categorized under the very high vulnerability category, found in residential areas and on stretches of dry sandy land (cells 1, 3-5, 7-19, and 24-28).

Meanwhile, gentle slopes ranged from 3.07% to 7.95% and were near settlements (cell 2), coastal tourism areas (cell 6), and mangrove forest areas (cells 20-21). The very high vulnerability on the Wini coast was found in rocky hill areas near highways (cells 22 and 23) and in the Tanjung Bastian area near the horserace (cells 29–30), with slopes of 19.58%, 19.49%, and 20.6% respectively. On the Oesoko coast, all observed cells (0.589%) were categorized having high vulnerability. Overall, the very high vulnerability category accounted for 43.58%, while the moderate vulnerability category was 23.07%, and the very low vulnerability category was 10.26%. Based on Tables 5, the very low vulnerability category comprised 10%, while the moderate and high vulnerability categories were 23% and 66.6%, respectively.

The elevation range of 0-5 meters was found across all cells on the Oesoko coast. On the Wini coast, this range was found in cell 8 (port area), cells 11-20 (near the settlements) and cells 24-28 (near the horserace area), all of which feature a flat slope. The elevation range of 5-10 meters was found in the settlements and along the highways, specifically in cells 1-10 on the Wini coast, where the slope ranges from gentle to flat. The elevation map is presented in Figure 6.

The highest elevation value was 11 meters, located at the village border near the horserace area (cells 29-30), where the slope was very steep at 20.5% and 20.6%. This high elevation could affect sea water inundation due to sea level rise. Some areas on the Wini coast, which are prone to significant standing water due to their low elevation, include the port area (cell 8), residential areas to the east of the mangrove forest area (cells 11-20), and the horserace area (cells 24-28). Sea water inundation due to sea level rise also has the potential to affect the entire coastal area of Oesoko Village. Figure 6 indicates that among the 39 observed cells, 28% were categorized as low vulnerability, while 5% fell under the moderate category, and 66.7% were deemed as very high vulnerability.

3.5. Relative Sea Level Rise

Based on spatial analysis, the highest sea level rise on the Wini coast was recorded at station 4, at 0.73 mm/year, while on the Oesoko coast, it was 0.83 mm/year. The average relative sea level rise in the waters of North Insana District was 0.78 mm/year, indicating that these waters were included in the low vulnerability class. The dynamics of relative sea level rise in North Insana waters is presented in Figure 7.

Table 5. Slope Classification on Wini Beach in 2023

Cell	Coordinate		Slope (%)	Slope Classification	Vulnerability Category
	X	Y			
1	663971	8985205	7.582	Flat	Moderate
2	668631	8984757	7.956	Gentle	Moderate
3	670667	8985244	0.05	Flat	Very High
4	673538	8986826	1.361	Flat	Very High
5	692327	8999531	3.098	Gentle	Moderate
6	692397	8999597	3.076	Gentle	Moderate
7	695972	9002395	0.104	Flat	Moderate
8	696099	9002549	0.639	Flat	Very High
9	696187	9002629	7.589	Gentle	Moderate
10	664069	8985183	7.589	Gentle	Moderate
11	664182	8985194	0.589	Flat	Very High
12	664326	8985163	0.589	Flat	Very High
13	664429	8985127	0.589	Flat	Very High
14	664509	8985102	0.589	Flat	Very High
15	664587	8985100	0.589	Flat	Very High
16	664696	8985177	0.589	Flat	Very High
17	664822	8985303	0.589	Flat	Very High
18	664927	8985374	0.589	Flat	Very High
19	665035	8985437	0.589	Flat	Very High
20	665189	8985440	7.812	Gentle	Moderate
21	665313	8985427	7.76	Gentle	Moderate
22	665488	8985416	19.589	Very Steep	Very Low
23	665553	8985390	19.49	Very Steep	Very Low
24	665656	8985349	0.589	Flat	Very High
25	665799	8985294	0.589	Flat	Very High
26	665892	8985245	0.589	Flat	Very High
27	665986	8985198	0.589	Flat	Very High
28	666118	8985144	0.589	Flat	Very High
29	666202	8985105	20.601	Very Steep	Very Low
30	666290	8985063	20.589	Very Steep	Very Low
31	666408	8985007	0.589	Flat	Very High
32	666512	8984961	0.589	Flat	Very High
33	666602	8984923	0.589	Flat	Very High
34	666669	8984966	0.589	Flat	Very High
35	666724	8984877	0.589	Flat	Very High
36	666853	8984850	0.589	Flat	Very High
37	666905	8984761	0.589	Flat	Very High
38	667026	8984714	0.589	Flat	Very High
39	667125	8984676	0.589	Flat	Very High

The north coast of Timor Island generally has a calm sea surface. According to Ledheng & Hano'e (2023), ocean areas with calm surfaces have relatively low energy patterns compared to other parts of the ocean. In addition, according to Suhana *et al*. (2016), archipelagic areas feature substantial landmasses that can reduce sea level rise. The relative sea level rise indicates how sea level changes affect specific parts of the shoreline. The change of sea surface height in North Insana District has a small spatial range because the data were collected from the same data stations along the shoreline. According to Koroglu *et al*. (2019), spatial variations of sea surface height changes typically occur in large areas. The range of sea level rise in North Insana District is lower than that observed in the waters of Biak Island, Papua Province, where it ranges from 1.57 to 1.97 mm/year (Rumahorbo *et al*., 2023).

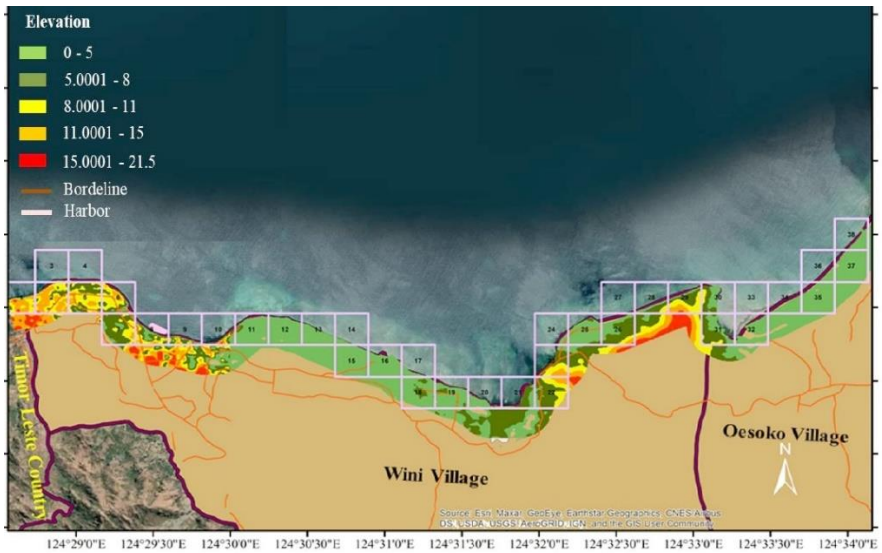

Figure 6. Map of Elevation in North Insana Distric

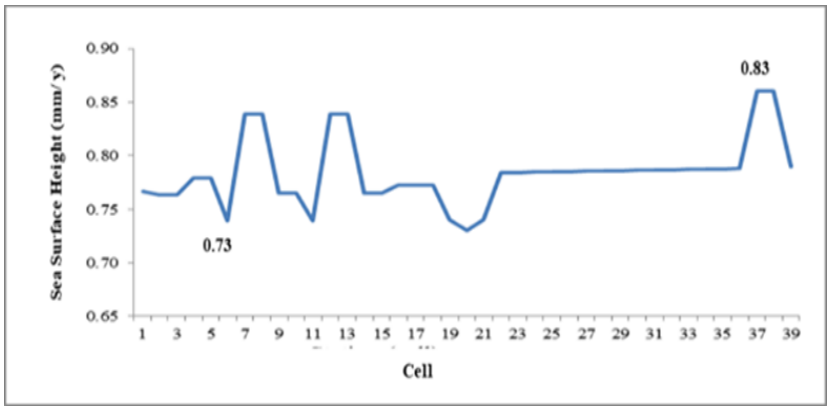

Figure 7. The Dynamics of Relative Sea Level Rise in North Insana Waters

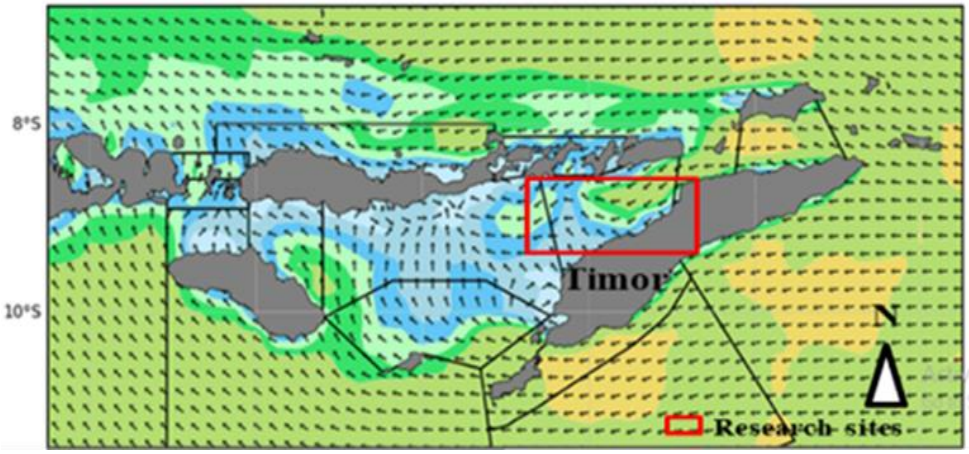

Figure 8. Wind Direction Recorded by BMKG in July 2023

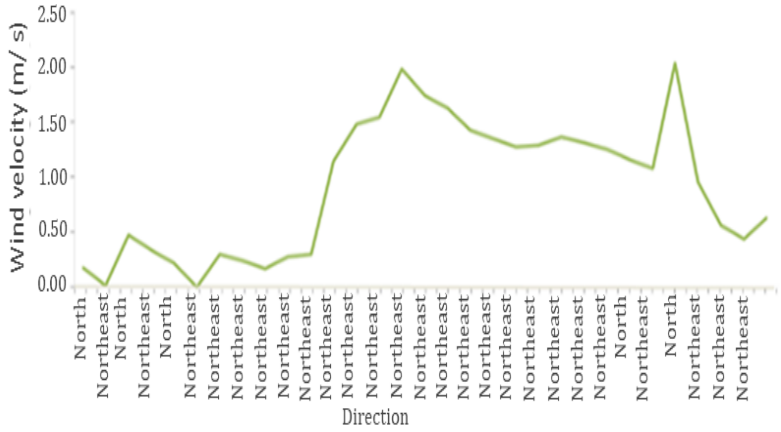

Figure 9. The Dominant Speed from Various Directions in the Waters of North Insana District in July 2023

3.6. Sea Wave Height

North Insana Beach is located in the Southern Hemisphere. The pattern of wind direction and speed in the southern hemisphere from May to August is strongly influenced by the east monsoon. This wind movement occurs during the first transitional season, shifting from the southeast to the northwest (Rifai *et al*., 2020). This is illustrated in the wind direction map of the waters off the northern part of Timor Island, recorded by the Meteorology, Climatology, and Geophysics Agency (BMKG), as presented in Figure 8.

The wind blows from the east, which tends to be dry as it travels from the south across a large desert area in the northern part of the Australian continent (Loupatty, 2013). The wind speed in the waters, as measured at North Insana as measured at the point of the fetch line (latitude: -8.9, longitude 124.66) is presented in Figure 9.

The dominant winds blow from the north and northeast, with speeds ranging from 0.05 to 2.18 m/s. The average wave height forecast for July 2023 was 0.27 m (Figure 10), with a maximum sea wave height of 0.1 m. (Figure 10), with a maximum sea wave height of 0.1 m.

The observed average wave height values represent 39 cells along the shoreline. Based on the vulnerability categorization by Lopez *et al*. (2016), wave heights below 0.65 m are considered very low vulnerability. In general, the wave height on the North Insana coast fell within the very low vulnerability category.

3.7. The Coastal Vulnerability of North Insana District

Spatially, the Coastal Vulnerability Index (CVI) to sea level rise on the coast of North Insana District fell in the low to moderate categories. The low category spanned 7.07 km (48.71%), while the moderate category covered 6.66 km (51.28%). The overall CVI value for North Insana District was 4.29, which was categorized as low vulnerability. This indicated the presence of several variables with low vulnerability that helped balance the high vulnerability of certain geological variables influencing the area. This finding aligned with the study Suhana *et al*. (2016), who found that low-vulnerability variables could act as counterbalancing factors in determining the overall level of coastal vulnerability. The spatial map of North Insana's coastal vulnerability is presented in Figure 11.

The level of CVI category can spatially describe the characteristics of vulnerability in a coastal area. If the vulnerability category varies, it is relative to the scale of the area assessed. Conversely, if it remains consistent throughout the shoreline, it shows that the category of vulnerability is regional or global in scope (Kasim & Siregar, 2012). Variables that influence the vulnerability of the North Insana coast included elevation, slope, geomorphology, and the rate of shoreline change. According to Hamuna *et al*. (2018), beach elevation is closely correlated with the coastal area's susceptibility to seawater inundation, while the beach slope is associated with the relative risk of inundation and can perform as the indicator of shoreline retreat's potential speed (Koroglu *et al*., 2019). This observation was consistent with the coastal conditions of North Insana District, which predominantly experienced abrasion, where slope and elevation had a significant effect on shoreline retreat. The development of residential areas on the North Insana coast was closely related to the activities of most fishermen, further influencing changes in the coastal environment. In addition, North Insana District receives special attention from the central government due to its status as a border area with Timor Leste, prompting development initiatives along its coastal areas. Therefore, the increase of human activity and development in the coastal areas possibly threatens the vulnerability in the coastal areas (Zonkouan *et al*., 2022).

In the study locations, there were no significant effects of oceanic physical variables (tides, wave height, and rate of sea level rise) on coastal vulnerability. However, as temporal variables, they could possibly have an essential impact in the future. It is predicted that the CVI value found in this study would likely change with the increasing intensity of infrastructure and settlement development in coastal areas.

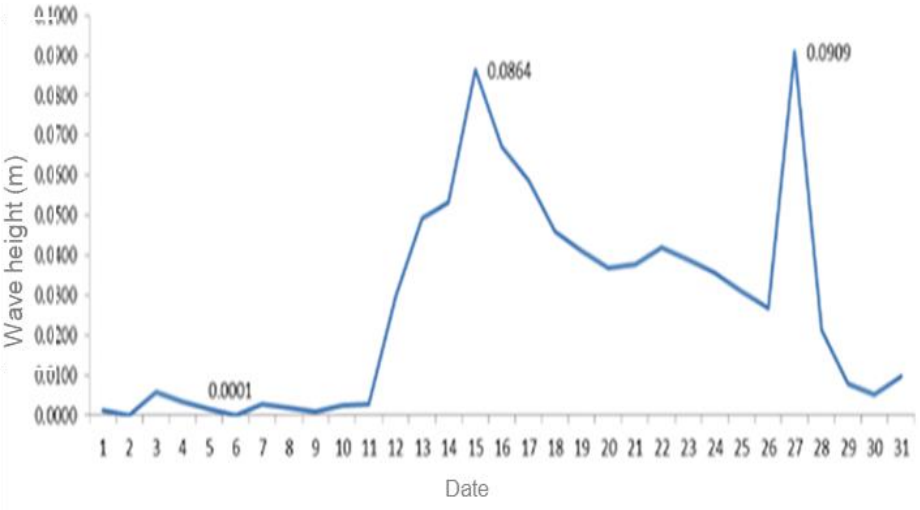

Figure 10. Daily Sea Wave Height in the Coastal Waters of North Insana

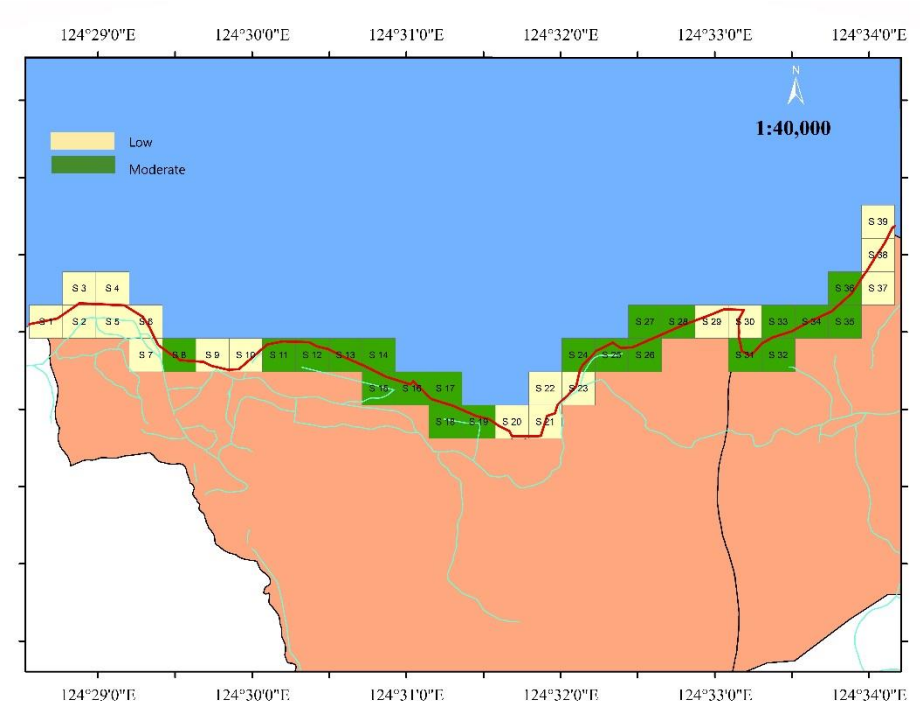

Figure 11. Coastal Vulnerability Map of North Insana District

4. CONCLUSION

This study produced a coastal spatial map of North Insana District with CVI values categorized as having a low to moderate risk of sea level rise. Based on the CVI values, the low category covered 7.07 km (48.71%), while the moderate category spanned 6.66 km (51.28%). The study results showed that the variables tides, wave height, and sea level rise were in low-vulnerability conditions and, therefore, did not have a significant effect on coastal vulnerability in the study area. However, as temporal variables, they could possibly have an imperative effect in the future.

The variables that affected the coastal vulnerability of North Insana District were geomorphology, slope, shoreline changes, and elevation. Geomorphology showed very high vulnerability (87.18%), the rate of shoreline change accounted for 7.6%, while slope and elevation contributed to very high vulnerability in 66.6% and 66.7% of the 39 cells observed. The limited number of variables used in this study could be a consideration in further research. For example, incorporation of additional aspects, such as socio-economy and the influence of human activities on the coastal environment, would acquire a more holistic CVI assessment. This approach could help coastal authorities and policymakers create more appropriate mitigation plans for potential disasters related to sea level rise.

ACKNOWLEDGMENTS

The researchers would like to thank the University of Timor through the Research and Community Service Institute for funding this research under the 2023 Basic Research Scheme (LPPM Basic Research No: 339/UN60/PP/2023).

REFERENCES

Copernicus. n.d. Welcome to the Climate Data Store. Accessed September 25, (2023). https://cds.climate.copernicus.eu/#!/home

Dipper, F., (2022). Chapter 2 - The seawater environment and ecological adaptations. Elements of Marine Ecology (Fifth Edition), Butterworth-Heinemann. Pages 37-151, https://doi.org/10.1016/B978-0-08-102826-1.00002-8.

DEMNAS.n.d. Download INAGEOPORTAL Accessed September 27, (2023). https://tanahair.indonesia.go.id/demnas.

Febriansyah, I., D. S, A. A., and Helmi, M. (2012). Kajian Kerentanan Pantai di Pesisir Kabupaten Cilacap, Jawa Tengah. Journal of Oceanography. 1(2): 139-148. https://ejournal3.undip.ac.id/index.php/joce/article/view/4153/4025

Hamuna, B., Sari, A. N., and Alianto, A. (2018). Kajian kerentanan wilayah pesisir ditinjau dari geomorfologi dan elevasi pesisir Kota dan Kabupaten Jayapura, Provinsi Papua. Jurnal Wilayah dan Lingkungan. 6(1): 1-14. http://dx.doi.org/10.14710/jwl.6.1.1-14

Jadidi A. (2013). Using geospatial business intelligence paradigm to design a multidimensional conceptual model for efficient coastal erosion risk assessment. Journal of coastal conservation. 17: 527–543. DOI: 10.1007/s11852-013-0252-5

Karondia, L. A., Handoko, E. Y., and Handayani, H. H. (2022). Analisa Kerentanan Pesisir Kota Semarang menggunakan algoritma CVI (Coastal Vulnerability Index). Geoid. 18(1): 99 111. DOI:10.12962/j24423998.v18i1.12969

Kasim F. and Siregar V.P. (2012). Coastal vulnerability assessment using integrated-method of CVI-MCA: a case study on the coastline of Indramayu. Forum Geografi. 26(1): 65 76. https://www.researchgate.net/publication/269409934

Koroglu, A., Ranasinghe, R., Jiménez, J. A., and Dastgheib, A. (2019). Comparison of coastal vulnerability index applications for Barcelona Province. Ocean & coastal management. 178: 1 13. DOI: 10.1016/j.ocecoaman.2019.05.001

Laming, S., & Rahim, M. (2020). Dampak pembangunan pesisir terhadap ekonomi dan lingkungan. Jurnal Sipil Sains, 10(2): 133 140. DOI: https://doi.org/10.33387/sipilsains.v10i2.2515

Ledheng, L., Ardhana, I. and Sundra, I., K. (2012). Komposisi dan struktur vegetasi mangrove di pantai Tanjung Bastian Kabupaten Timor Tengah Utara Propinsi Nusa Tenggara Timur. Ecotrophic. 4(2): 80 85. https://ojs.unud.ac.id/index.php/ECOTROPHIC/article/view/2535

Ledheng, L., Naisumu, Y., G., and Binsasi, R. (2020). Kajian biomassa dan cadangan karbon pada hutan mangrove pantai utara kabupaten timor tengah utara Provinsi Nusa Tenggara Timur. Prosiding Seminar Nasional Inergitas Multidisiplin Ilmu Pengetahuan dan Teknologi. 3(1): 217 229. https://jurnal.yapri.ac.id/index.php/semnassmipt/article/view/166

Ledheng, L., and Hano'e, E. M. Y. (2023). Analysis of Shoreline Change of North Central Timor Regency, Indonesia. Nature Environment & Pollution Technology. 22(2): 777 787. DOI:10.46488/NEPT.2023.v22i02.020

Li, J.T., Liu, Y.S., Yang, Y.Y. 2018. Land Use Change and Effect Analysis of Tideland Reclamation in Hangzhou Bay. Journal of Mountain Science, 15(2), 394-405.

López Royo, M., Ranasinghe, R., and Jiménez, J. A. 2(016). A rapid, low-cost approach to coastal vulnerability assessment at a national level. Journal of Coastal Research. 32(4): 932 - 945. DOI: 10.2112/JCOASTRES-D-14-00217.1

Loupatty, G. (2013). Karakteristik energi gelombang dan arus perairan di Provinsi Maluku. BAREKENG: Jurnal Ilmu Matematika dan Terapan. 7(1): 19 22. Doi:10.30598/barekengvol7iss1pp19-22

Nurrohmah, E., Sunarto, S., & Khakhim, N. (2016). Pemilihan lokasi kawasan konservasi mangrove dengan pendekatan SIG partisipatif di wilayah pantai Kabupaten Demak. Majalah Geografi Indonesia, 30(2), 149-169.

Pendleton E.A., Thieler E.R., and Williams S.J. (2010). Importance of coastal change variables in determining vulnerability ti sea-and lake-level change. Journal of Coastal Research. 26(1): 176 - 183. DOI: 10.2112/08-1102.1

Rifai, A., Rochaddi, B., Fadika, U., Marwoto, J. and Setiyono, H. (2020). Kajian Pengaruh Angin Musim Terhadap Sebaran Suhu Permukaan Laut (Studi Kasus: Perairan Pangandaran Jawa Barat). Indonesian Journal of Oceanography. 2(1): 98 104. DOI:10.14710/ijoce.v2i1.7499

Rumahorbo, B. T., Warpur, M., Tanjung, R. H., and Hamuna, B. (2023). Spatial Analysis of Coastal Vulnerability Index to Sea Level Rise in Biak Numfor Regency (Indonesia). Journal of Ecological Engineering. 24(3): 113 - 125. DOI: 10.12911/22998993/157539

Sakka, S., Paharuddin, P., and Rupang, E. (2014). Analisis Kerentanan Pantai Berdasarkan Coastal Vulnerability Index (CVI) di Pantai Kota Makassar. Torani Journal of Fisheries and Marine Science. 24(3): 49 53. DOI:10.35911/torani.v24i3.237

Siregar, R. H. (2016). Pengaruh Kerapatan Mangrove terhadap Laju Sedimen Transpor di Wilayah Pesisir Desa Pulau Sembilan Kabupaten Langkat Sumatera Utara (Doctoral dissertation, Universitas Sumatera Utara).

Suhana, M. P., Nurjaya, I. W., and Natih, N. M. N. (2016). Analisis kerentanan pantai timur pulau Bintan menggunakan digital shoreline analysis dan coastal vulnerability index. Jurnal Teknologi Perikanan dan Kelautan. 7(1): 21 - 38. DOI: 10.24319/jtpk.7.21-38

Suhana, M. P., Putra, R. D., Shafitri, L. F., Muliadi, M., Khairunnisa, K., Nurjaya, I. W., & Natih, N. M. N. (2020). Tingkat Kerentanan Pesisir di Utara dan Timur Pulau Bintan Provinsi Kepulauan Riau Tahun 2020. Jurnal Teknologi Perikanan dan Kelautan. 11(1): 11 - 27. Doi: 10.24319/jtpk.11.11-27

Yuliastini, L. F., Zainuri, M., & Widiaratih, R. (2023). Analisis Kerentanan Pesisir di Kabupaten Kendal. Indonesian Journal of Oceanography. 5(1): 80-89. DOI: 10.14710/ijoce.v5hi1.16061

Zonkouan B.R.V., Bachri I., Beda A.H.J., N'Guessan K.A.M. (2022). Monitoring Spatial and Temporal Scales of Shoreline Changes in Lahou-Kpanda (Southern Ivory Coast) Using Landsat Data Series (TM, ETM+ and OLI). Geomatics and Envi- ronmental Engineering. 16(1): 145 - 158. DOI: 10.7494/geom.2022.16.1.145